

Savings in locomotor adaptation explained by changes in learning parameters following initial adaptation

Firas Mawase,¹ Lior Shmuelof,² Simona Bar-Haim,³ and Amir Karniel¹

¹Department of Biomedical Engineering, Ben-Gurion University of the Negev, Beer-Sheva, Israel; ²Department of Brain and Cognitive Sciences, Ben-Gurion University of the Negev, Beer-Sheva, Israel; and ³Department of Physical Therapy, Ben-Gurion University of the Negev, Beer-Sheva, Israel

Submitted 15 October 2013; accepted in final form 13 January 2014

Mawase F, Shmuelof L, Bar-Haim S, Karniel A. Savings in locomotor adaptation explained by changes in learning parameters following initial adaptation. *J Neurophysiol* 111: 1444–1454, 2014. First published January 15, 2014; doi:10.1152/jn.00734.2013.—Faster relearning of an external perturbation, savings, offers a behavioral linkage between motor learning and memory. To explain savings effects in reaching adaptation experiments, recent models suggested the existence of multiple learning components, each shows different learning and forgetting properties that may change following initial learning. Nevertheless, the existence of these components in rhythmic movements with other effectors, such as during locomotor adaptation, has not yet been studied. Here, we study savings in locomotor adaptation in two experiments; in the first, subjects adapted to speed perturbations during walking on a split-belt treadmill, briefly adapted to a counter-perturbation and then readapted. In a second experiment, subjects readapted after a prolonged period of washout of initial adaptation. In both experiments we find clear evidence for increased learning rates (savings) during readaptation. We show that the basic error-based multiple timescales linear state space model is not sufficient to explain savings during locomotor adaptation. Instead, we show that locomotor adaptation leads to changes in learning parameters, so that learning rates are faster during readaptation. Interestingly, we find an intersubject correlation between the slow learning component in initial adaptation and the fast learning component in the readaptation phase, suggesting an underlying mechanism for savings. Together, these findings suggest that savings in locomotion and in reaching may share common computational and neuronal mechanisms; both are driven by the slow learning component and are likely to depend on cortical plasticity.

computational motor control; locomotor adaptation; motor learning; split-belt

OUR MOTOR SYSTEM IS KNOWN for its ability to rapidly adapt to changes in the environment and changes of its own (Scheidt et al. 2000; Thoroughman and Shadmehr 2000). It was suggested that such adaptation depends on an error-based process that gradually updates one's controller based on the discrepancy between forward model predictions and sensory inputs (e.g., sensory prediction errors) (Shadmehr and Mussa-Ivaldi 1994). For example, when humans start to walk on split-belt treadmill imposing different speeds to each leg, the sensory consequences of the motor commands are different than expected, causing kinematic (Reisman et al. 2005) and kinetic (Mawase et al. 2013) motor errors. Exposed to such perturbation, subjects gradually modulate the walking speed of each leg to adapt to the speed imposed by the treadmill. Interestingly, this

learning process led to the formation of a motor memory that can be recalled later (Malone et al. 2011; Shadmehr and Brashers-Krug 1997).

Faster relearning of the same perturbation when introduced again (i.e., savings) receives great attention in the motor control community since it reflects the formation of a new motor memory. Initial attempts to model adaptation to an external perturbation were based on state space models (SSMs) composed of a fast and one or multiple slow processes (Lee and Schweighofer 2009; Smith et al. 2006). However, these linear multiple-rate SSMs could not explain savings that occur after a prolonged period of washout (Krakauer et al. 2005; Zarahm et al. 2008) and across days (Robinson et al. 2006). Instead, a recently nonlinear SSM (Zarahm et al. 2008) and context-dependent models (Ingram et al. 2011; Lee and Schweighofer 2009) were suggested to better explain a variety of phenomena reported in the motor adaptation literature, including savings. While evidence for savings has been accumulated from different systems [saccades, arm reaching, and locomotion (Kojima et al. 2004; Krakauer et al. 2005; Malone et al. 2011)] and across paradigms [saccades, visuomotor; and force field adaptation (Kojima et al. 2004; Krakauer et al. 2005; Smith et al. 2006; Zarahm et al. 2008)], adaptation and savings were mainly modeled based on reaching and saccades adaptation results and, to the best of our knowledge, were never modeled for locomotor adaptation. The generalization of adaptation models which were constructed based on reaching experiments to locomotor adaptation is questionable, as the two behaviors differ greatly in terms of neuronal substrates, the nature of the behavior, and the role of visual feedback: locomotion is rhythmic, depends greatly on central pattern generators located in the spinal cord, and shows adaptation at the spinal cord level (Heng and de Leon 2007), whereas reaching movements are discrete, guided by visual input, and depend on cortical substrates.

Recently, savings in locomotor adaptation was reported in a set of psychophysical experiments (Malone et al. 2011). In these studies savings across days was found even after a washout of initial learning, suggesting that savings in locomotion reflect enhanced learning and not residual state components. Nevertheless, locomotor adaptation was never formally modeled using SSMs, and the nature of parameter changes following initial adaptation has not been examined yet.

Commonalities between the computational components leading to adaptation and savings of reaching and locomotor adaptation may shed light on the neuronal and mechanistic basis of motor savings.

Address for reprint requests and other correspondence: A. Karniel, Biomedical Engineering Dept., Ben Gurion Univ. of the Negev, P.O. Box 653 Beer Sheva, 84105 Israel (e-mail: akarniel@bgu.ac.il).

Here we investigate the computational basis of locomotor adaptation by comparing the performance of a linear dual-rate SSM with SSMs with changing parameters (Zarahn et al. 2008), under the hypothesis that locomotor adaptation leads to changes in learning parameters that would last beyond the decay of the hidden state of the system. Furthermore, we were interested in the relationship between the initial and second adaptation phases, hypothesizing that the magnitude of savings will be correlated with the learning achieved during the initial exposure to adaptation. Recent results suggest that long-term retention (savings) is affected by the slow learning process (Joiner and Smith 2008) and that the slow process may be sensitive to reward whereas the fast process is not (Huang et al. 2011). Furthermore, Berniker and Kording (2011) recently suggested that the fast and slow processes represent assignment of the source of the error to internal and external perturbations, respectively. All these perspectives suggest that savings may be the outcome of a slow learning and slow decaying process. By fitting slow and fast learning components to the adaptation and readaptation phases independently, we can investigate the relationship between the above learning parameters.

The current study has two main aims. The first is to study the nature of savings in locomotor adaptation by comparing linear and nonlinear SSMs. The second aim was to explore the relationship of the slow and fast learning components before and after learning.

MATERIALS AND METHODS

Subjects. Forty subjects (23 males, 17 females, mean age: 25.9 ± 2.7 yr) participated in the current study. All subjects were naïve to our paradigm, without neurological history and without known disturbances in walking. All subjects signed the informed consent form as stipulated by the Institutional Helsinki Committee, which reviewed and approved all protocols.

Apparatus and general experimental procedure. Subjects were instructed to walk on a custom split-belt force treadmill (ForceLink, Clemborg, The Netherlands), which has two separate belts and an embedded force plate (Fig. 1A). The speed and the direction (forward vs. backward) of each treadmill belt were controlled independently. The belt speed could be in one of two conditions, either moving together at same speed (tied-belts) or moving separately at different speeds (split-belts).

Subjects were positioned in the middle of the split-belt treadmill with one foot on each belt. They were instructed to look straight forward, preventing the usage of available visual feedback from the environment regarding the speeds of the belts. For safety, all subjects wore a safety harness that was suspended from the ceiling, and two emergency stop buttons were available during the experiment and two adjustable side bars were available to prevent falls. The safety harness and the side bars did not support the subjects during the experiments. Custom software written in C# (Microsoft Visual Studio) was used for controlling the speed of the belts and the timing of the experiments.

Center of pressure (COP) data were sampled and recorded using Gaitfors software (ForceLink). The system recorded the COP data at 500 Hz using one-dimension force sensors from a single large (160×800 mm) force plate embedded in the treadmill. COP is defined as the

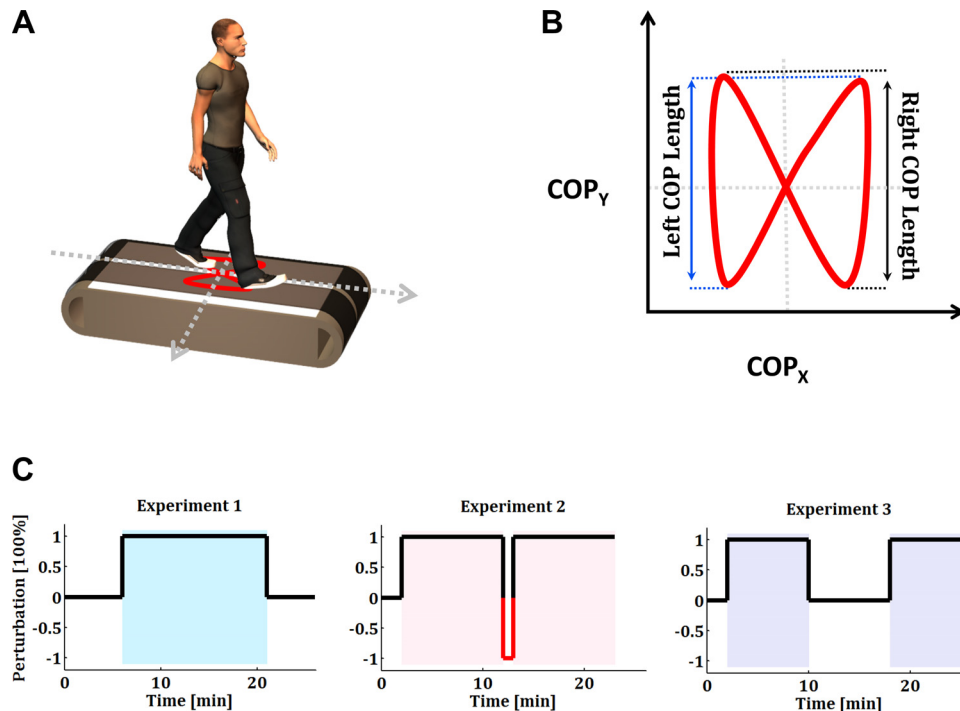


Fig. 1. Experimental design and protocols. **A:** subjects walked on a split-belt force treadmill with 2 separated belts and an embedded force plate (white plate). Red trace represents the center of pressure (COP) profile for 1 gait cycle. **B:** schematic example for 1 COP profile for 1 cycle. Left COP length was calculated as the y (anterior-posterior) distance in the COP profile between consecutive left toe off (TO) and right initial contact (IC) and right COP length was calculated as the y distance between consecutive right TO and left IC. **C, left:** protocol of *experiment 1*: baseline (6 min), adaptation (15 min), and washout (5 min). During the baseline block, subjects walked with both belts at same speed (tied-belts) [0.5:0.5 m/s (2 min), 1:1 m/s (2 min), and 0.5:0.5 m/s (2 min)]. During adaptation, subjects walked with different speeds (split-belts) (0.5:1 m/s). During washout, subjects walked on tied-belts at slow speed condition (0.5:0.5 m/s). **Middle:** protocol of *experiment 2*: baseline (2 min), adaptation (10 min), counterperturbation (30 s), and readaptation (10 min). During the baseline block, subjects walked on tied-belts [0.6:0.6 m/s (1 min) and 1.2:1.2 m/s (1 min)]. During adaptation, subjects walked on split-belts (0.6:1.2 m/s; slow belt under dominant leg). During counterperturbation, the belts were set to the opposite split-belts pattern (1.2:0.6 m/s). All subjects were then reexposed to the same split-belts, as in the adaptation block, again for 10 min, (0.6:1.2 m/s; slow belt under dominant leg). **Right:** protocol of *experiment 3*: baseline (2 min), adaptation (8 min), washout (8 min), and readaptation (8 min). Speed condition in each block of *experiment 3* was similar to *experiment 2*.

projection of the resultant vertical force vector on the ground plane (Benda et al. 1994). Determining the two coordinates (x and y) of the COP is based on measuring the force component from each force transducer placed on the corner of the force platform (Besser et al. 1993). The system was also able to determine representative gait events such as initial contact (IC) and toe off (TO) for each leg independently (Roerdink et al. 2008). In this study, our primary adaptation measurement was *COP symmetry*, which has previously been shown as a robust adaptation index (Mawase et al. 2013). COP symmetry was defined as follows:

$$\text{COP symmetry} = \frac{\text{left COP length} - \text{right COP length}}{\text{left COP length} + \text{right COP length}} \quad (1)$$

where left COP length was calculated as the y (anterior-posterior) distance in the COP profile between consecutive left TO and right IC and right COP length was calculated as the y distance between consecutive right TO and left IC (Fig. 1B). The difference was then normalized to the sum of the right and left COP length.

Our aim was to understand what drives adaptation and savings during locomotion. Predominantly, we aimed to test the learning process that underlies locomotor adaptation. To answer this question, we began with reanalyzing previously collected data from Mawase et al. (2013) (*experiment 1*). We followed up with two additional experiments (*experiments 2 and 3*) in which we tested the best variation of the SSM that explains savings during locomotor adaptation.

Experiment 1: adaptation-washout paradigm. For *experiment 1* adaptation-washout (AW), we reanalyzed data of 10 subjects (6 males, 4 females, mean age, 25.8 ± 3.4 years) from a dataset previously reported by Mawase et al. (2013). For all subjects, the self-identified dominant leg was the right leg. Leg dominance was determined by asking each subject about the leg he/she uses to kick a ball. All subjects completed three blocks: *baseline*, *adaptation*, and *washout* (Fig. 1C, left). During the baseline block, subjects walked with both belts at same speed for 6 min. They started with the “slow” speed, then at “fast” speed, and, finally, at “slow” speed for 2 min at each speed. We define “slow” and “fast” speeds to be 0.5 m/s and 1 m/s, respectively. During adaptation, subjects walked with the belts of the split-belt treadmill moving at different speeds for each leg for 15 min. The belt of the left (nondominant) leg moved always at the slow speed while the belt of the right leg moved at the fast speed. During washout, the belts were set again to move together at the slow speed (0.5 m/s) for 5 min.

The aim of reanalyzing the AW experiment was to test whether the traditional single/dual-rate SSM (Smith et al. 2006), designed to study reaching adaptation, could also account for locomotor adaptation. In particular, the purpose was to test whether the models can capture the shape of the error reduction and the aftereffect curves seen following removal of the perturbation (i.e., washout).

Experiment 2: adaptation-counterperturbation-readaptation paradigm. Seventeen naïve subjects (10 males, 7 females, mean age 26.1 ± 1.8 yr) participated in *experiment 2*. For 16 subjects, the self-identified dominant leg was the right leg. Subjects in the counterperturbation experiment completed four walking blocks: *baseline*, *adaptation*, *adaptation to counterperturbation*, and *readaptation* (Fig. 1C, middle). All subjects experienced 2 min of baseline walking on tied-belts. They walked 1 min at “slow” speed (0.6 m/s) followed by another one min at “fast” speed (1.2 m/s). All subjects were then adapted to split-belts (belts split at 0.6 and 1.2 m/s; slow belt under dominant leg) for 10 min. Subjects were then briefly adapted with opposite split-belts (belts split at 1.2 and 0.6 m/s; fast belt under dominant leg) for 30 s. All subjects were then readapted to the split-belts presented at the first adaptation block, again for 10 min (belts split at 0.6 and 1.2 m/s; slow belt under dominant leg).

Experiment 3: adaptation-washout-readaptation paradigm. Thirteen naïve subjects (7 males, 6 females, mean age 25.7 ± 1.9 yr) with

right dominant leg participated in *experiment 3*. Subjects in the washout experiment completed four walking blocks: *baseline*, *adaptation*, *washout*, and *readaptation* (Fig. 1C, right). All subjects experienced 2 min of baseline walking on tied-belts. Then they walked 1 min at “slow” speed (0.6 m/s) followed by another one min at “fast” speed (1.2 m/s). All subjects were then adapted to split-belts (belts split at 0.6 and 1.2 m/s; slow belt under dominant leg) for 8 min. Subjects were then washed out with the slow tied-speed (belts tied at 0.6 m/s) for 8 min. All subjects were then readapted to the same split-belts presented in the first adaptation block (belts split at 0.6 and 1.2 m/s; slow belt under dominant leg) for 8 min.

Modeling. Different variations of the SSM have been recently suggested to explain adaptation and savings during force field (Donchin et al. 2003; Smith et al. 2006), object rotation (Ingram et al. 2011), and visuomotor (Lee and Schweighofer 2009; Zarahn et al. 2008) perturbations. Most of these models assume linear time invariant (LTI) properties of the parameters (Donchin et al. 2003; Ingram et al. 2011; Lee and Schweighofer 2009; Smith et al. 2006) while the rest model assumes varying parameters that change with experience (Berniker and Kording 2011; Zarahn et al. 2008). All of these error-based models suggest that trial-by-trial adaptation occurs by updating the appropriate internal models (i.e., states) to reflect the behavior of the perturbation. However, the varying parameter (VP) model suggests that motor adaptation occurs by updating the parameters along with the states. In the current study, we compare the prediction of three variations of the proposed SSM during locomotor adaptation: 1) dual-rate LTI SSM (Smith et al. 2006), 2) single-rate varying parameters SSM (Zarahn et al. 2008), and 3) dual-rate varying parameters SSM (Zarahn et al. 2008). The equations of the models took the following forms:

1) Dual-rate SSM:

$$\begin{aligned} e(n) &= D \cdot f(n) - y(n) \\ y(n) &= x_f(n) + x_s(n) \\ x_f(n+1) &= A_f \cdot x_f(n) + B_f \cdot e(n) \\ x_s(n+1) &= A_s \cdot x_s(n) + B_s \cdot e(n) \\ A_f &< A_s < 1, B_s < B_f < 1 \end{aligned}$$

2) Single-rate varying parameters SSM:

$$\begin{aligned} e(n) &= D \cdot f(n) - y(n) \\ y(n) &= x_f(n) \\ x(n+1) &= A(p) \cdot x(n) + B(p) \cdot e(n) \end{aligned}$$

3) Dual-rate varying parameters SSM:

$$\begin{aligned} e(n) &= D \cdot f(n) - y(n) \\ y(n) &= x_f(n) + x_s(n) \\ x_f(n+1) &= A_f(p) \cdot x_f(n) + B_f(p) \cdot e(n) \\ x_s(n+1) &= A_s(p) \cdot x_s(n) + B_s(p) \cdot e(n) \\ A_f(p) &< A_s(p) < 1, B_s(p) < B_f(p) < 1 \end{aligned}$$

In a given trial n , $e(n)$ is the motor error, $f(n)$ is the external perturbation (defined as the difference between left and right belt speeds), and $y(n)$ is the net motor output on the same trial (i.e., the state of the learner). $A(p)$ and $B(p)$ are the forgetting and learning rate constants that change with an experience p , respectively. *Experiments 2 and 3* contain three experience phases: adaptation-counterperturbation-readaptation in *experiment 2* and adaptation-washout-readaptation in *experiment 3*. D is a compliance scalar with units of seconds per meter. The *dual-rate SSM* suggests that the net motor output has two inner states $x_f(n)$ and $x_s(n)$, where $x_f(n)$ is the fast process that reacts rapidly to motor error but has weak memory retention and $x_s(n)$ is the slow process that reacts slowly to motor error but significantly exhibits strong retention. To this end, it contains five free constant parameters (A_f, B_f, A_s, B_s, D). In the *single-rate varying parameters SSM*, there is only single learning process $x(n)$, which has varying forgetting and learning parameters $A(p)$ and $B(p)$, respectively. This model contains seven free parameters [$A_{\text{adaptation}}, B_{\text{adaptation}}, A_{\text{deadaptation}}, B_{\text{deadaptation}}, A_{\text{readaptation}}, B_{\text{readaptation}}, D$] and [$A_{\text{adaptation}}, B_{\text{adaptation}}, A_{\text{washout}}, B_{\text{washout}}, A_{\text{readaptation}}, B_{\text{readaptation}}, D$] for *experiments 2 and 3*, respectively. Finally, the *dual-rate varying parameters SSM*, which has 13 free parameters, suggests that the net motor output has a single state

in the fast process and a single state in the slow process for each experience phase (i.e., adaptation/counterperturbation/washout/readaptation). In addition, the motor output/perturbation [i.e., $y(n)/f(n) = 1 - e(n)/f(n)$] represents the predicted amount of adaptation in each trial.

We searched for the best model that simultaneously accounts for adaptation and savings during locomotion. Model selection was performed by the Akaike Information Criterion (AIC) (Akaike 1974), computed for the single subject data. For each candidate model, the AIC value reflects the combination of fitting amount along with the number of free parameters, and the optimal model is identified by the minimum value of AIC. Thus the difference in AIC values of two candidate models would provide strong indication toward the best fitting model.

$$\text{AIC} = 2 \cdot k - n \cdot \ln(L) \quad (2)$$

where k is the number of free parameters, n is the number of data points, and L is the maximized value of the likelihood function for the estimated model. Under the assumption that the model errors are independent and identically normally distributed, we can rewrite the criterion as follow:

$$\text{AIC} = 2 \cdot k + n \cdot \ln(\sigma_r^2) \quad (3)$$

where σ_r is the standard deviation of the residual errors between the actual and predicted data. AIC analysis is critical for our study to account for the increase in number of free parameters introduced in the varying parameters SSM models.

We estimated the parameters of the models by using the *fmincon* routine performed by Matlab that maximized the log likelihood. In all experiments, the estimated error of each model was fitted to the individual subject's data. In *experiments 2* and *3*, the estimated error was fitted simultaneously to all three phases. Thereafter, we calculated the mean and the standard error for each parameter in each experiment phase for further comparison analysis.

For each adaptation and readaptation phase and for each individual subject, we quantified the initial error as the motor error of the first trial and mid-error as the average of the trials 2–30. This method has previously been shown as a robust savings measurement index (Malone et al. 2011). Following the definition of savings by previous works as an increase in the rate of error reduction following initial learning (Huang et al. 2011; Malone et al. 2011; Zarahn et al. 2008), we fit a single exponential function, which has the form $y(n) = a \cdot e^{-n/b} + c$, to each subject's data to estimate the rate of error reduction. Moreover, savings was also quantified as the difference between mid-errors across the two adaptation blocks. In addition, we defined “initial bias” as the difference between initial errors across the two adaptation blocks.

Statistical analysis. Statistical analysis of the data was performed using the Matlab software with Statistics Toolbox (The MathWorks,

Natick, MA). We used repeated-measure analyses of variance (ANOVA_{RM}) to compare differences between AIC values of the models in *experiments 2* and *3*. When significant differences were found, post hoc analyses were performed. The Shapiro-Wilk *W*-test with an alpha level of 0.05 was used to assess the *t*-test assumption of normality on the AIC difference values across subjects. When the *P* value was greater than the chosen alpha level, a paired *t*-test was used to compare the difference in AIC between models. Otherwise, nonparametric Wilcoxon matched-pair signed-rank test was used for comparison. Correlation between learning parameters (i.e., B_f and B_s) and motor errors was evaluated using the Pearson correlation coefficients. The free parameters and their confidence intervals of the single exponential function were estimated using the Matlab software with the Curve Fitting Toolbox. A two-tailed *t*-test was used to compare initial error and mid-error in *experiments 2* and *3*. Significance level was set to 0.05.

RESULTS

Experiment 1: learning processes in locomotor adaptation. We first sought to test the hypothesis whether basic LTI single-rate or dual-rate learning process could explain the fundamental principles of locomotor adaptation time course, i.e., the error reduction during the perturbation block and, predominantly, the aftereffect during the washout block. To this end, we reanalyzed our previous published data (Mawase et al. 2013). Figure 2A shows the learning process during adaptation to speed perturbation using the split-belt system. During the baseline phase (i.e., zero perturbation), COP symmetry (i.e., motor error) values were close to zero, mean error at the baseline phase across subjects was 0.007 ± 0.042 (means \pm SD), which indicates a symmetric pattern of locomotion. During early adaptation, there was a significant positive value of the error. The mean error over the first two trials was 0.56 ± 0.077 (means \pm SD). This positive value of error decreased slowly throughout the adaptation phase, reaching an error rate of 0.128 ± 0.046 over the last 10 trials. In the early postadaptation phase (washout), there was a clear negative aftereffect, indicated by mean error of -0.57 ± 0.079 over the first two trials. This reverse pattern gradually returned to baseline values, reaching error value of -0.067 ± 0.047 over the last 10 trials.

We fit the single-rate SSM as well as the dual-rate SSM to the trial series of the motor error for each subject from *experiment 1*. The single-rate model has one state, whereas the dual-rate model proposed that the motor output has two inde-

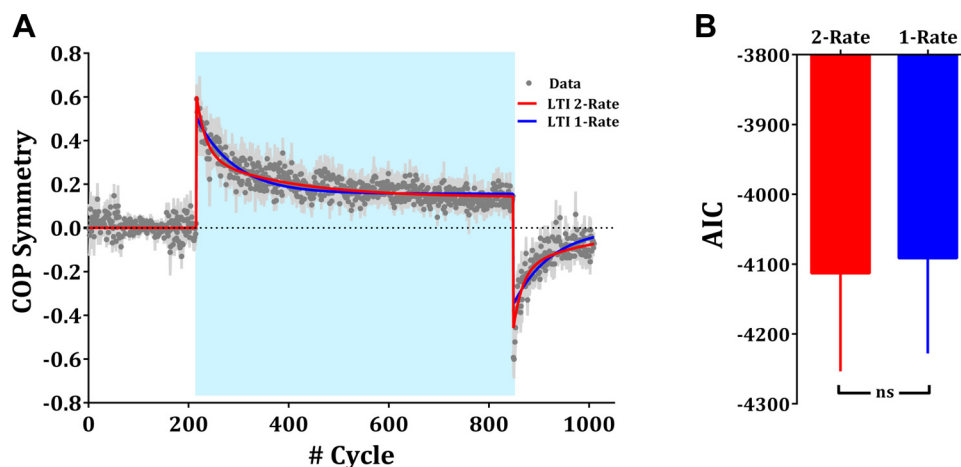


Fig. 2. Group data and model prediction during *experiment 1*. A: across-subject averaged COP symmetry (gray points) in each gait cycle and the fitted linear time invariant (LTI) single-rate state space model (SSM) (blue line) and dual-rate SSM (red line). B: across-subject averaged Akaike Information Criterion (AIC) for the single-rate SSM (blue bar) and for the dual-rate SSM (red bar), respectively. Error bars indicate SE.

pendent states, a fast state that reacts rapidly to motor error but has strong forgetting rate, and one slow state that reacts slowly to motor error but significantly exhibits strong retention (see MATERIALS AND METHODS). Since there is only one adaptation phase in *experiment 1*, the single-rate LTI model is identical to the single-rate varying parameters model. The two SSMs models were computed separately for each subject and simultaneously to all phases of the experiment. The across-subject averages of the parameter estimates from the single-rate SSM were $A = 0.9939 \pm 0.0017$ (means \pm SE), $B = 0.0153 \pm 0.0047$, and $D = 1.0944 \pm 0.1429$, and the across-subject averages of the parameter estimates from the dual-rate SSM were $A_{\text{fast}} = 0.6885 \pm 0.1367$ (means \pm SE), $A_{\text{slow}} = 0.9979 \pm 0.0009$, $B_{\text{fast}} = 0.01781 \pm 0.0827$, $B_{\text{slow}} = 0.0094 \pm 0.0023$, and $D = 1.3958 \pm 0.1115$. To qualitatively illustrate the time courses of the different SSMs during *experiment 1*, we fitted the two models to the across-subject averaged data (Fig. 2A). As shown in Fig. 2A, the two models did a responsible job of explaining adaptation and aftereffect during the first experiment.

To select the best model, we used the AIC to account for the different number of parameters in each model. For each candidate model, the AIC value reflects the combination of the goodness of fitting along with the number of free parameters. That is, the AIC difference between two candidate models would provide strong evidence in favor of the model with the lower AIC value. To assess the normality assumption of the t -test on the AIC difference values across subjects, we used the Shapiro-Wilk W -test. We found that the W value was insignificant at alpha level of 0.05, suggesting that the assumption of normality of the AIC distribution is valid ($W = 0.92$, $P > 0.39$). Figure 2B shows the mean AIC across subjects for each model. The AIC of the dual-rate SSM (-4112.9 ± 140.6 ,

means \pm SE) was comparable to the AIC of the single-rate model (-4091.4 ± 136.5 , means \pm SE). The t -statistic reveals that no difference was observed in the AIC of the two models [two-tailed paired t -test, $t(9) = 1.83$, $P = 0.11$], indicating that both models fit well the behavioral data of the first experiment. However, neither savings nor anterograde interference can be examined in this type of experimental paradigm. Therefore, we designed two additional experiments to test these phenomena.

Experiment 2: savings in counterperturbation paradigm. In the second experiment, we sought to quantify within-day savings effects and to find whether the single-rate or the dual-rate SSM, which showed a good fit to single phase locomotor adaptation, can also explain the faster relearning phenomenon (e.g., savings). To this end, we asked subjects to relearn the same split-belt perturbation after a brief counterperturbation period that erased the initial adaptation (Fig. 3A). During counterperturbation phase, the error of the last five strides was on average -0.64 ± 0.04 (means \pm SE), which is not significantly different [$t(16) = 0.986$, $P = 0.3385$] from the magnitude of the -0.6 counter perturbation [defined as the difference between left (0.6 m/s) and right (1.2 m/s) belt speeds]. This result indicates that subjects had completely erased their initial adaptation but did not start adapting to the counterperturbation. Subjects exhibited strong savings during relearning of the same perturbation. Mid-error during readaptation, computed based on strides 2–30 (0.22 ± 0.04 , means \pm SE), was significantly lower [two-tailed paired t -test, $t(16) = 8.96$, $P < 0.0001$] than the mid-error during adaptation (0.47 ± 0.03). That is, following initial adaptation, subjects learned the perturbation significantly faster (Fig. 3B), indicating the existence of savings. Furthermore, we measured the effect of savings by estimating directly the learning rates during adap-

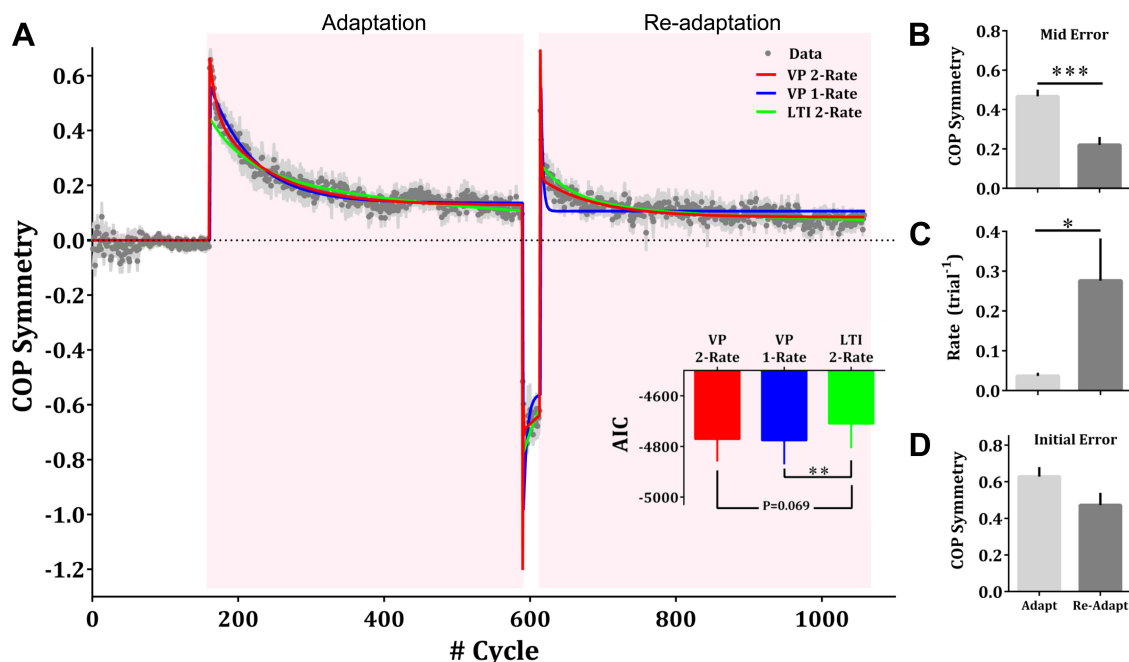


Fig. 3. Group data and models predictions during *experiment 2*. A: across-subject averaged COP symmetry (gray points). Colored lines represent the fits of the SSM models: green line represents the prediction of the LTI dual-rate SSM, blue line represents the prediction of the varying parameters (VP) single-rate SSM, and red line represents the prediction of the varying parameters dual-rate SSM. Inset: across-subject averaged AIC for each model, respectively. B: mid-errors averaged across subjects during adaptation (light gray bar) and readaptation (dark gray bar). C: average learning rate of a single exponential fit to individual subject data from adaptation (light gray bar) and readaptation (dark gray bar). D: initial errors averaged across subjects during adaptation (light gray bar) and readaptation (dark gray bar). Error bars indicate SE. * $P < 0.05$; *** $P < 0.001$.

tation and readaptation before and after adaptation. Indeed, the learning rate of the exponential function in the readaptation block ($0.28 \pm 0.1 \text{ trial}^{-1}$) was higher [$t(16) = 2.24, P < 0.05$] than the learning rate of the initial adaptation block ($0.04 \pm 0.008 \text{ trial}^{-1}$; Fig. 3C). We could not find evidence for initial bias; analyzing the error of the first trial revealed that there was no difference in COP symmetry between adaptation and readaptation [$t(16) = 1.66, P = 0.12$; Fig. 3D].

Three alternative models of the behavioral data in *experiment 2* were compared. The first was the LTI multiple time-scales (i.e., LTI 2-Rate), which has two states, one fast and one slow (see MATERIALS AND METHODS). The second was the single-rate varying parameters SSM (i.e., VP 1-Rate), which has a single learning process that has forgetting and learning parameters that could vary across phases. The last one was the dual-rate varying parameters SSM (i.e., VP 2-Rate), which has single state in the fast process and single state in the slow process with varying forgetting and learning parameters. The VP models were fitted for each phase separately, namely: one fit for adaptation, one for counterperturbation, and one for the readaptation phase. The three SSMs models were computed separately for each subject and simultaneously to all three phases of the experiment. The across-subject averages of the parameter estimates are provided in Table 1. To qualitatively illustrate the time courses of the different SSMs during *experiment 2*, we fitted the three models to the across-subject averaged data (Fig. 3A). As shown in Fig. 3A, the LTI 2-Rate SSM did a responsible job of explaining adaptation and savings

during readaptation. Although the VP 1-Rate SSM did a good job explaining adaptation, it explained poorly savings during readaptation, yielding too rapid readaptation. VP 2-Rate SSM fit well the averaged data overall.

To select the best model, we again used the AIC to account for the different number of parameters in each model. The Shapiro-Wilk *W*-test on the AIC differences across subjects reveals that none of the *W* values was significant, suggesting weak evidence to reject the null hypothesis of normally distributed population ($P > 0.47$). Figure 3A, *inset*, shows the mean AIC across subjects for each model. ANOVA showed main effect of model on AIC measures ($F_{2,16} = 4.87, P < 0.05$). The AIC of the VP 1-Rate SSM ($-4,776.2 \pm 23.0$, means \pm SE) was significantly lower [two-tailed paired *t*-test, $t(16) = 3.46, P < 0.01$] than that of the LTI 2-Rate SSM ($-4,710.0 \pm 30.9$). The AIC of the VP 2-Rate SSM ($-4,770.9 \pm 21.6$) tended toward being favored [two-tailed paired *t*-test, $t(16) = 1.95, P = 0.069$] over the LTI 2-Rate SSM.

To summarize *experiment 2*, the models with changing parameters between adaptation and readaptation explain the performance of single subjects better than the canonical two-rate SSM.

Experiment 3: savings in washout paradigm. In the third experiment, we examined whether completely erasing the learned pattern by exposing subjects to a prolonged washout period would affect future locomotor savings and whether one of the candidate SSM models could account for that. To this end, we asked subjects to relearn after a prolonged washout period (Fig. 4A). Comparing the mean errors of the last five strides of the washout phase (0.011 ± 0.03 , means \pm SE) and the mean errors of the last five strides of the baseline phase (0.014 ± 0.01 , means \pm SE) showed no significant differences in error rates [two-tailed paired *t*-test, $t(12) = 0.08, P > 0.9$], indicating that subjects had completely returned to their baseline performance. Subjects demonstrated strong savings when they were reexposed to the same perturbation for the second time. The mid-error during readaptation (0.36 ± 0.04 , means \pm SE) was significantly lower [two-tailed paired *t*-test, $t(12) = 9.04, P < 0.0001$] than the mid-error during adaptation (0.59 ± 0.04 , means \pm SE). Therefore, savings (i.e., the difference between the mid-errors) is significantly evident in the adaptation-washout-readaptation experiment [one-sample *t*-test, $t(12) = 9.04, P < 0.001$; Fig. 4B]. Estimating the learning rate of a single exponent function revealed similar results. We found that the estimated learning rate of the exponential function in the readaptation phase ($0.06 \pm 0.01 \text{ trial}^{-1}$) was higher [$t(12) = 3.5, P < 0.01$] than the time learning rate of the initial adaptation ($0.04 \pm 0.004 \text{ trial}^{-1}$; Fig. 4C). Consistent with *experiment 2*, analyzing the error of the first trial revealed that there was no difference in COP symmetry between adaptation and readaptation [$t(12) = 1.94, P = 0.08$; Fig. 4D].

Similarly to *experiment 2*, the three suggested SSMs models were computed separately for each subject and simultaneously in all three phases of the experiment. The across-subject averages of the parameter estimates are also provided in Table 1. To qualitatively illustrate the time courses of the different SSMs during *experiment 3*, we fitted the three models to the across-subject averaged data (Fig. 4A). As shown in Fig. 4A, the LTI 2-Rate SSM and the VP 1-Rate SSM could not capture the savings phenomenon during readaptation, whereas the VP 2-Rate SSM fit the averaged data very well overall.

Table 1. Across-subject averages of the SSM parameters during phase 1 (i.e., adaptation) and phase 3 (i.e., readaptation) of *experiment 2* and 3

	VP Dual-Rate	VP Single-Rate	LTI Dual-Rate
<i>Experiment 2</i>			
<i>Phase 1</i>			
A_{fast}	$0.4254 \pm (0.1061)$	N/A	$0.4403 \pm (0.099)$
A_{slow}	$0.9962 \pm (0.001)$	$0.9952 \pm (0.001)$	$0.9986 \pm (0.001)$
B_{fast}	$0.1006 \pm (0.035)$	N/A	$0.0861 \pm (0.036)$
B_{slow}	$0.0241 \pm (0.005)$	$0.0227 \pm (0.005)$	$0.0092 \pm (0.002)$
D	$1.2740 \pm (0.047)$	$1.0511 \pm (0.062)$	$0.8191 \pm (0.045)$
<i>Phase 3</i>			
A_{fast}	$0.7147 \pm (0.0590)$	N/A	N/A
A_{slow}	$0.9724 \pm (0.0155)$	$0.9445 \pm (0.019)$	N/A
B_{fast}	$0.3283 \pm (0.0596)$	N/A	N/A
B_{slow}	$0.0837 \pm (0.0263)$	$0.3120 \pm (0.065)$	N/A
D	$1.2740 \pm (0.047)$	$1.0511 \pm (0.062)$	N/A
<i>Experiment 3</i>			
<i>Phase 1</i>			
A_{fast}	$0.2011 \pm (0.0976)$	N/A	$0.4778 \pm (0.1245)$
A_{slow}	$0.9965 \pm (0.0008)$	$0.9959 \pm (0.0008)$	$0.9949 \pm (0.0016)$
B_{fast}	$0.0739 \pm (0.0394)$	N/A	$0.0646 \pm (0.0242)$
B_{slow}	$0.0134 \pm (0.0023)$	$0.0134 \pm (0.0024)$	$0.0139 \pm (0.0032)$
D	$1.3078 \pm (0.0688)$	$1.1871 \pm (0.0676)$	$1.2086 \pm (0.0597)$
<i>Phase 3</i>			
A_{fast}	$0.6103 \pm (0.0837)$	N/A	N/A
A_{slow}	$0.9879 \pm (0.0037)$	$0.9767 \pm (0.0052)$	N/A
B_{fast}	$0.2222 \pm (0.0379)$	N/A	N/A
B_{slow}	$0.0395 \pm (0.0115)$	$0.0756 \pm (0.0171)$	N/A
D	$1.3078 \pm (0.0688)$	$1.1871 \pm (0.0676)$	N/A

Values are means with SE in parentheses. VP Dual-Rate, varying parameters dual-rate state space model (SSM); VP Single-Rate, varying parameters single-rate SSM; LTI, linear time invariant; *A*, forgetting rate constant; *B*, learning rate constant; *D*, compliance scalar with units of seconds per meter; N/A, parameter not applicable for that model.

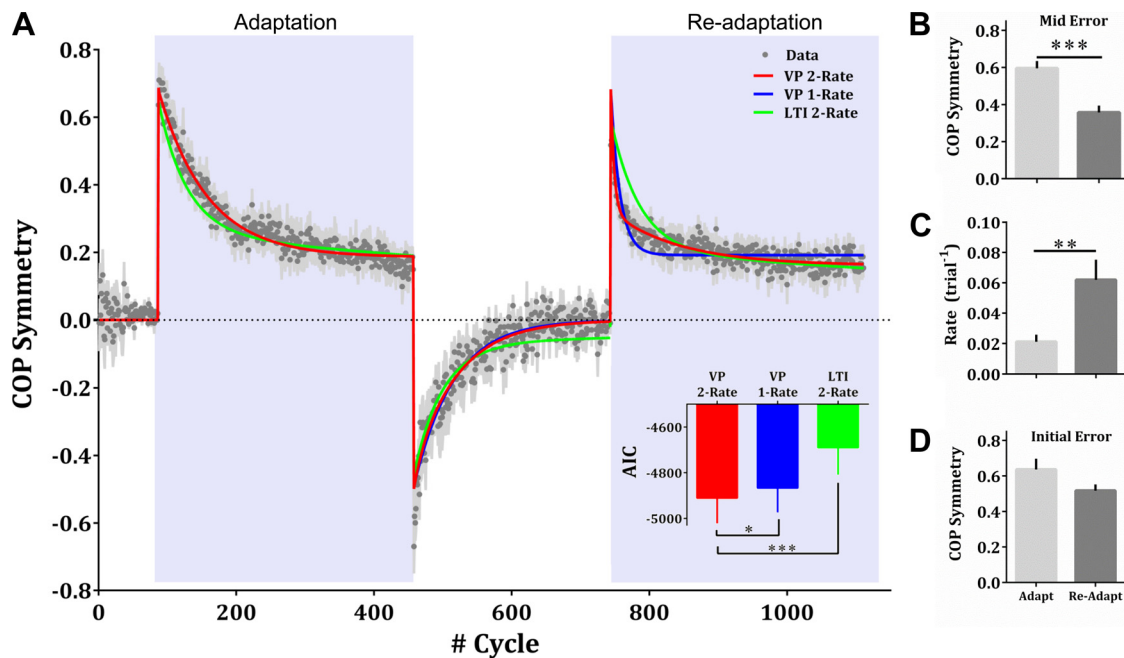


Fig. 4. Group data and models predictions during *experiment 3*. *A*: across-subject averaged COP symmetry (gray points). Color lines represent the fits of the SSM models: green line represents the prediction of the LTI dual-rate SSM, blue line represents the prediction of the varying parameters single-rate SSM, and red line represents the prediction of the varying parameters dual-rate SSM. *Inset*: across-subject averaged AIC for each model, respectively. *B*: mid-errors averaged across subjects during adaptation (light gray bar) and readaptation (dark gray bar). *C*: average learning rate of a single exponential fit to individual subject data from adaptation (light gray bar) and readaptation (dark gray bar). *D*: initial errors averaged across subjects during adaptation (light gray bar) and readaptation (dark gray bar). Error bars indicate SE. * $P < 0.05$; ** $P < 0.01$; *** $P < 0.001$.

Figure 4A, *inset*, shows the mean AIC across subjects for each model. To assess data normality, we used the Shapiro-Wilk W -test on the AIC differences across subjects. We found two out of three W values were insignificant ($P > 0.08$), indicating that these differences are probably normally distributed. However, the W value of the AIC differences between VP 2-Rate and VP 1-Rate was significant ($P = 0.02$). To this end, we follow with nonparametric Wilcoxon matched pair signed-rank test to compare the difference between VP 2-Rate with VP 1-Rate. ANOVA showed main effect of model on AIC measures ($F_{2,12} = 15.64$, $P < 0.01$). We found that the AIC of the VP 2-Rate SSM ($-4,911.5 \pm 30.7$, means \pm SE) was significantly lower [two-tailed paired t -test, $t(12) = 4.692$, $P < 0.001$] than that of the LTI 2-Rate SSM ($-4,690.0 \pm 32.9$). Additionally, the AIC of the VP 2-Rate SSM was significantly lower (Wilcoxon matched pair signed-rank test, $P = 0.01$) than that of the VP 1-Rate SSM (-4867.3 ± 29.6).

To summarize *experiment 3*, the dual-rate model with changing parameters between adaptation and readaptation after a prolonged period of washout explains the performance of single subjects significantly better than the canonical LTI dual-rate model and the varying parameters single-rate model.

Parameter changes associated with savings. Following the initial stages of model selection, showing that VP 2-Rate SSM explains savings effects better in *experiment 3*, we asked which parameters change following initial learning in both experiments. Figure 5A shows the slow and fast state estimates from the VP 2-Rate SSM to the across-subject averaged data during *experiment 2*. Both learning rates (i.e., B_f and B_s) and forgetting rates (i.e., A_f and A_s) changed following adaptation. Analyzing the across-subject averages of the parameter estimates reveals that the forgetting rate of the fast state (i.e., A_f) in adaptation (0.43 ± 0.1 , means \pm SE) was significantly

lower [two-tailed t -test, $t(32) = 2.384$, $P < 0.05$] than the forgetting rate of the fast state in readaptation (0.71 ± 0.06 ; Fig. 5B), whereas the change of the forgetting rate of the slow state (i.e., A_s) was not significant [two-tailed t -test, $t(32) = 1.526$, $P = 0.14$] across blocks (0.99 ± 0.01 and 0.97 ± 0.02 in adaptation and readaptation, respectively; Fig. 5C). Moreover, the learning rate of the fast state (i.e., B_f) in adaptation (0.1 ± 0.04) was significantly increased [two-tailed t -test, $t(32) = 3.291$, $P < 0.01$] during readaptation (0.33 ± 0.06 ; Fig. 5D), and the learning rate of the slow state (i.e., B_s) in adaptation (0.024 ± 0.01 , means \pm SE) was significantly increased [two-tailed t -test, $t(32) = 2.223$, $P < 0.05$] during readaptation (0.08 ± 0.03 ; Fig. 5E).

A similar picture is seen in *experiment 3* (Fig. 6A), where both learning and forgetting rates of the slow and fast learning components have changed. The forgetting rate of the fast state (i.e., A_f) in adaptation (0.20 ± 0.1 , means \pm SE) was significantly lower [two-tailed t -test, $t(24) = 3.182$, $P < 0.01$] than the forgetting rate of the fast state in readaptation (0.61 ± 0.08 ; Fig. 6B), and the forgetting rate of the slow state (i.e., A_s) in adaptation (0.996 ± 0.001) was also significantly higher [two-tailed t -test, $t(24) = 2.305$, $P < 0.05$] than the forgetting rate of the slow state in readaptation (0.987 ± 0.02 ; Fig. 6C). Moreover, the learning rate of the fast state (i.e., B_f) in adaptation (0.07 ± 0.04) was significantly increased [two-tailed t -test, $t(24) = 2.714$, $P < 0.05$] during readaptation (0.22 ± 0.04 ; Fig. 6D), and the learning rate of the slow state (i.e., B_s) in adaptation (0.013 ± 0.002 , means \pm SE) was also significantly increased [two-tailed t -test, $t(24) = 2.23$, $P < 0.05$] during readaptation (0.04 ± 0.01 ; Fig. 6E). From the fits of the averaged data presented in Fig. 6A, it seems that the adaptation process could be captured by only a single slow state with no contribution of a fast state. Nevertheless, learning rates from

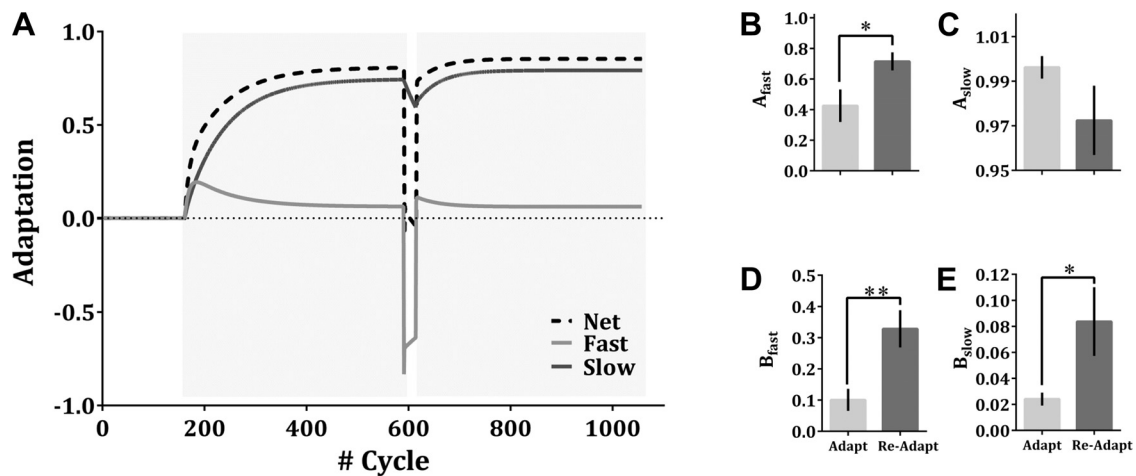


Fig. 5. Adaptation of the slow and fast components of the varying parameters dual-rate SSM during *experiment 2*. **A**: net (dashed black line), slow (dark gray line), and fast state (light gray line) estimates from the VP 2-Rate SSM to the across-subject averaged data. **B**: forgetting rates of the fast process (i.e., A_{fast}) averaged across subjects during adaptation (light gray bar) and readaptation (dark gray bar). **C**: forgetting rates of the slow process (i.e., A_{slow}) averaged across subjects during adaptation (light gray bar) and readaptation (dark gray bar). **D**: learning rates of the fast process (i.e., B_{fast}) averaged across subjects during adaptation (light gray bar) and readaptation (dark gray bar). **E**: learning rates of the slow process (i.e., B_{slow}) averaged across subjects during adaptation (light gray bar) and readaptation (dark gray bar). Error bars indicate SE. * $P < 0.05$; ** $P < 0.01$.

the single-subject fits of the fast components of the adaptation phase tend to be higher than zero [$t(12) = 2.1$, $P = 0.06$ for A_f and $t(12) = 1.9$, $P = 0.08$ for B_f], suggesting that across subjects, the fast component did play a role in the initial adaptation block.

Although initial bias did not reach significance levels, there was a trend towards a decrease in initial error in readaptation compared with adaptation in both experiments (Figs. 3D and 4D). To obviate a possible bias influence on the estimation of learning parameters in our models during the readaptation phase, we have added a free parameter in our varying parameters model that represents an initial bias (e.g., a possible bias effect) during readaptation. Consistent with our previous results, we found similar changes in learning parameters following initial learning. Adding this additional parameter did not affect the AIC results favoring the VP models. Thus our suggested model is robust for possible bias effects.

Correlation of savings, adaptation, and learning parameters. Previous attempts to explain savings used a LTI model with two learning components (LTI 2-Rate SSM), showing that the slow forgetting of the slow learning component can account for various savings phenomena (Smith et al. 2006). Nevertheless, consistently with the results of Zarahn et al. (2008), we show here that also in locomotor adaptation, models with varying parameters account better for savings effects in adaptation-counterperturbation-readaptation and adaptation-washout-readaptation paradigms, suggesting that different learning parameters are expressed before and after learning. Still, the fact that learning parameters change through learning does not mean that they are independent; it could be that the changes in parameters following learning are correlated with their initial values. Such dependency will be indicative of the mechanisms that give rise to savings. We therefore investigated the correlation of error rates and learning parameters as seen in the

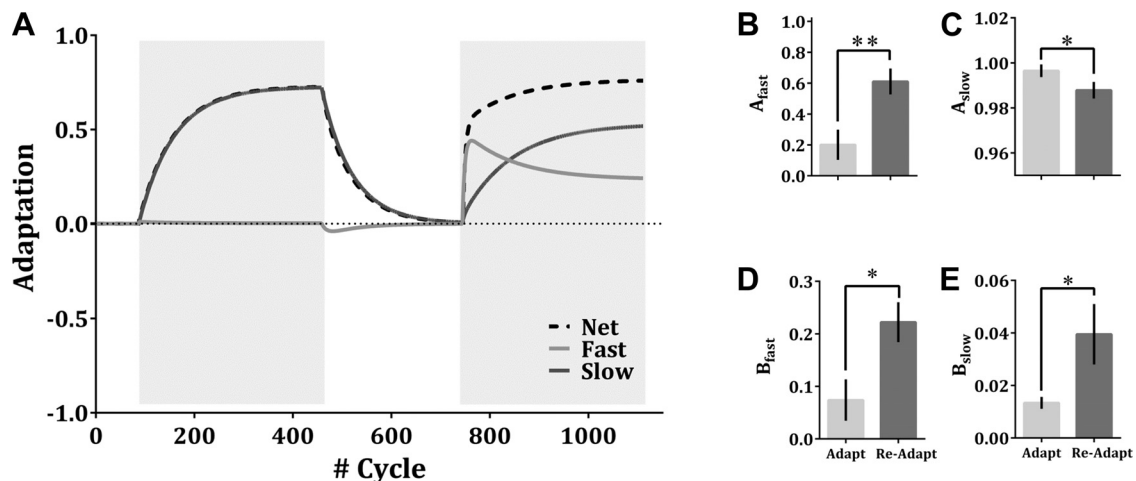


Fig. 6. Adaptation of the slow and fast components of the varying parameters dual-rate SSM during *experiment 3*. **A**: net (dashed black line), slow (dark gray line), and fast state (light gray line) estimates from the VP 2-Rate SSM to the across-subject averaged data. **B**: forgetting rates of the fast process (i.e., A_{fast}) averaged across subjects during adaptation (light gray bar) and readaptation (dark gray bar). **C**: forgetting rates of the slow process (i.e., A_{slow}) averaged across subjects during adaptation (light gray bar) and readaptation (dark gray bar). **D**: learning rates of the fast process (i.e., B_{fast}) averaged across subjects during adaptation (light gray bar) and readaptation (dark gray bar). **E**: learning rates of the slow process (i.e., B_{slow}) averaged across subjects during adaptation (light gray bar) and readaptation (dark gray bar). Error bars indicate SE. * $P < 0.05$; ** $P < 0.01$.

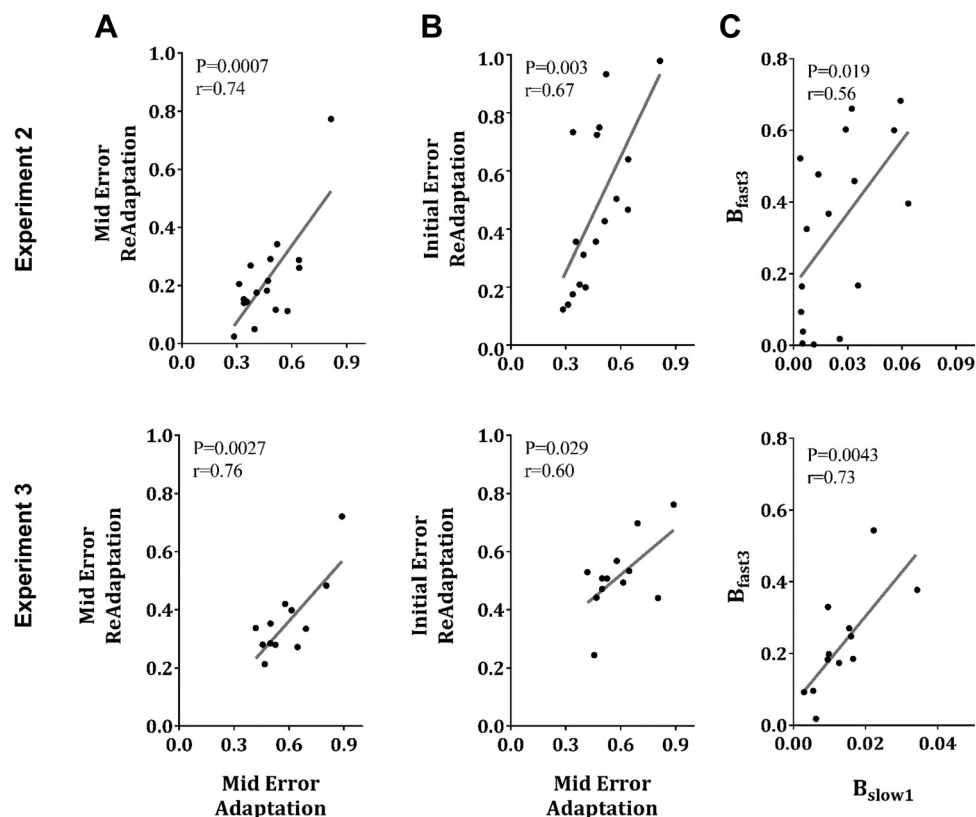
intersubject correlation patterns between adaptation and readaptation blocks. We started by examining the intersubject correlation of the initial and middle error rates in the adaptation and readaptation phases. We found that both initial errors and middle errors in readaptation significantly correlated with middle errors in the adaptation phase (all comparisons reveal $0.60 \leq r \leq 0.76$ and $0.0007 \leq P \leq 0.029$, Fig. 7, A and B), indicating that early readaptation is correlated with subjects' behavior during the initial adaptation phase. We then moved to examining the correlation pattern of the estimated learning parameters that could potentially provide a refined estimation of the source of correlation that we have seen in error rates. We found that out of the four possible pairs of learning rate correlations (slow and fast adaptation rates vs. slow and fast readaptation rates) in each experiment, only the slow adaptation and fast readaptation learning parameters were significantly correlated in both experiments [$r = 0.56$, $P = 0.019$ (Pearson correlation test) for *experiment 2* (Fig. 7C, top) and $r = 0.73$, $P = 0.0043$ for *experiment 3* (Fig. 7C, bottom), respectively]. In both tests there are four comparisons that require correcting for false positive rates. Applying these corrections using Bonferroni correction results in a significant effect for the slow adaptation and fast readaptation learning parameters for *experiment 3* and a marginal result for *experiment 2* ($P = 0.019$ where the corrected threshold was 0.0125). Nevertheless, the consistency of results in the two experiments and across the two measurements (of error rates and learning parameters) suggests that the correlation between readaptation learning and the slow initial adaptation is not spurious. Another concern about the current correlation results is that while the correlations between middle errors in adaptation and readaptation epochs were significant, the correlations of the slow learning parameters (i.e., B_s) in

both these periods were not. At this point we cannot tell whether this apparent inconsistency is a due to the fact that the middle error correlations is driven by the correlation between the slow and fast learning parameters in the adaptation and readaptation epochs, respectively, or due to our limited sensitivity to detect correlations between the slow learning parameters in the two epochs.

DISCUSSION

Using the split-belt treadmill paradigm, we examined the learning mechanisms underlying adaptation and savings during the learning of a novel locomotor task. In the first experiment, we reanalyzed our previous results (Mawase et al. 2013) to establish the computational model of the basic learning process within a simple adaptation paradigm. However, the data from the first experiment missed an important phenomenon of motor learning: savings. Therefore, we designed two additional experiments to test for savings effects. Based on several experimental paradigms developed for reaching adaptation (Krakauer et al. 2005; Smith et al. 2006; Zarah et al. 2008), we chose the adaptation-counterperturbation-readaptation (i.e., *experiment 2*) and the adaptation-washout-readaptation (i.e., *experiment 3*) protocols to test the underlying learning process for savings. We found that while multiple-rate SSM can account for initial error reduction and aftereffects of the simple adaptation paradigm (i.e., *experiment 1*), it failed to explain savings in the second and the third experiments. Instead, we found that allowing the parameters of the dual-rate state space learning process to change following initial learning can successfully explain savings effects seen in both protocols. This supports the hypothesis that locomotor adaptation leads to changes in the fast and slow learning parameters that would last beyond

Fig. 7. Correlation of the errors and learning parameters during *experiments 2 and 3*. A: cross-correlation between middle errors in adaptation and middle errors in readaptation during *experiment 2* (top) and *experiment 3* (bottom). B: cross-correlation between middle errors in adaptation and initial errors in readaptation during *experiment 2* (top) and *experiment 3* (bottom). C: cross-correlation between the slow adaptation parameter (i.e., B_{slow1}) and fast readaptation learning parameter (i.e., B_{fast3}) estimate from the VP 2-Rate SSM during *experiment 2* (top) and *experiment 3* (bottom).



the decay of the hidden state of the motor system. Furthermore, analyzing the intersubject variability provides a suggestive causal relationship between the slow and fast learning components before and after learning, respectively. Particularly, we found that the fast relearning rate depends on the slow learning rate during adaptation, suggesting that the magnitude of savings will be proportional to the learning achieved during the prolonged exposure to adaptation. Together, these findings shed new insights into the formation of motor memory.

Our model-comparison results are consistent with a recent study where savings effects in reaching visuomotor adaptation paradigms were examined (Zarahn et al. 2008). Zarahn et al. (2008) suggested a nonlinear time invariant SSM to properly account for savings during the readaptation phase. This nonlinear behavior underlies the metalearning process by allowing changes in the learning parameters in an experience-dependent manner. A key aspect of the model is that consequent adaptation phases are associated with adjustable learning and forgetting rates. We found significantly different learning and forgetting parameters across the phases of an adaptation experiment (Figs. 5 and 6). Suggestive changes in learning parameters can also be seen in a recent locomotor adaptation study, where Malone et al. (2011) found that different adaptation structures affect significantly the retention of the motor memory during readaptation on the subsequent day. The faster relearning rate on the subsequent day provides evidence of the involvement of a nonlinear learning process in locomotor adaptation. While the results of Malone were not modeled, we show here that indeed a LTI model cannot account for several within-day savings phenomena and provide a suggestive underlying mechanism for this effect.

Recently, context-dependent linear models with either single or multiple slow states have been suggested to explain savings during visuomotor rotation (Lee and Schweighofer 2009), force-field adaptation (Pekny et al. 2011), and object rotation (Ingram et al. 2011). According to the context-dependent learning approach, motor adaptation occurs through a fast and a slow contextual learning process that is updated simultaneously by the same motor errors. Savings occurs by switching back to a previously learned internal model (slow process). A noticeable limitation of the context-dependent model is that it does not account for consolidation after learning (Criscimagna-Hemminger and Shadmehr 2008) or adaptation across days (Kording et al. 2007). The fact that all the slow states decay with time needs to be refined, as subjects clearly retain across days (Malone et al. 2011). Furthermore, the changes in the fast learning process following adaptation suggest that savings cannot be explained only by the changes in slow learning processes and requires modification of the fast process as well, a property that does not exist in the current context-dependent learning approach. Together, our behavioral and computational results strongly lead to the conclusion that savings occurs through changes in learning parameters (meta-learning) and not by switching between hidden learning states.

Although individuals learn differently a given motor task in terms of learning rates, most of the previous studies focused on averaged learning rates measured across subjects, leaving the intersubject variability completely unexplored. In the current study, we studied the relationship between the slow and fast learning components before and after learning. Using VP-2 SSM parameters, we found a significant correlation between

the slow learning rate during adaptation and the fast learning rate during readaptation (Fig. 7). These results are also found when looking at the correlation between initial and middle errors during adaptation and during readaptation phases. Thus the magnitude of savings for each subject was proportional to the learning achieved by the slow learning process. These findings suggest that even though the varying parameters model accounted for our result better than the fixed parameter model, learning parameters during adaptation and readaptation are not independent and may be subjected to a higher learning process that modulates the learning parameters following learning. Our interpretation of the positive correlation between the fast state during readaptation and the slow state during initial adaptation is that savings is predominantly the outcome of a slow learning and slow decaying process of initial adaptations. This conclusion is consistent with recent works that emphasize the role of the slow process in long-term retention (Joiner and Smith 2008), in estimation of the source of error (Kording et al. 2007), and in savings in force field adaptation (Smith et al. 2006).

Despite multiple differences between reaching and locomotor adaptation, we found that learning in both behaviors can be explained using the same VP models and, in both paradigms, savings depend on the slow learning process. Thus a reasonable conjecture is that the two learning behaviors also share a similar neuronal basis. Two predominant brain areas are likely to be involved in adaptation learning: cerebellum and motor cortex (Shmuelof and Krakauer 2011). Several studies suggested that the cerebellum is involved in error-based learning (Atkeson 1989; Diedrichsen et al. 2005; Kawato et al. 1987; Miall et al. 2007), and damage to the cerebellum hampers the ability to adapt to external perturbations based on sensory prediction errors (Ilg et al. 2008; Maschke et al. 2004; Morton and Bastian 2004, 2006; Tseng et al. 2007). Recently, Jayaram et al. (2012) used a noninvasive transcranial magnetic stimulation to show that the cerebellum excitability is modulated during locomotor adaptation. Furthermore, Galea et al. (2011) found that noninvasive stimulation using tDCS over the cerebellum enhances error-reduction during visuomotor reaching adaptation task. Interestingly, this stimulation did not affect subsequent savings. Thus the cerebellum is needed for adaptation learning in reaching and locomotion and is likely to affect the rate of the learning. The motor cortex, on the other hand, has been shown to be involved in retention of adaptive patterns (savings) but not directly in adaptation, as patients with stroke in the motor systems can adapt (Reisman et al. 2007; Scheidt et al. 2000; Scheidt and Stoeckmann 2007). In the same study of Galea et al. (2011), stimulation over the primary motor cortex did not change the learning rate of reaching adaptation but increased its subsequent savings. Taken together, while the cerebellum is likely to be vital for the fast learning process, we speculate that the savings in our study depends on primary motor cortex processes that are likely to affect behavior through the slow learning process. The fact that we did find correlations between the slow learning process and the fast relearning process suggests that the two learning processes are not independent. It remained to be seen whether the enhancement of the fast process is retained in the cerebellum or is the result of the feedforward control over the locomotion pattern controlled by the cortex or by the controller itself, located in the cortex and the spinal cord.

We conclude that adaptation and savings in locomotion occur through modulation of learning parameters in a dual-rate model. These changes are consistent with results in reaching adaptation, suggesting a common mechanism for savings, which is likely to depend on the motor cortex. It would be interesting to investigate our within-day savings results with savings across days to further elucidate the dynamics of parameter changes following initial adaptation.

GRANTS

This work was supported by the U.S. Agency for International Development (USAID), the Middle East Regional Cooperation Program (MERC), Grant No. 74/12 from the Israel Science Foundation (ISF), and the Ministry of Science and Technology, Israel.

DISCLOSURES

No conflicts of interest, financial or otherwise, are declared by the author(s).

AUTHOR CONTRIBUTIONS

Author contributions: F.M., S.B.-H., and A.K. conception and design of research; F.M. performed experiments; F.M. analyzed data; F.M., L.S., S.B.-H., and A.K. interpreted results of experiments; F.M. prepared figures; F.M. drafted manuscript; F.M., L.S., S.B.-H., and A.K. edited and revised manuscript; F.M., L.S., S.B.-H., and A.K. approved final version of manuscript.

REFERENCES

- Akaike H.** A new look at the statistical model identification. *IEEE Trans Automat Contr* 19: 716–723, 1974.
- Atkeson CG.** Learning arm kinematics and dynamics. *Annu Rev Neurosci* 12: 157–183, 1989.
- Benda BJ, Riley P, Krebs D.** Biomechanical relationship between center of gravity and center of pressure during standing. *IEEE Trans Rehabil Eng* 2: 3–10, 1994.
- Berniker M, Kording KP.** Estimating the relevance of world disturbances to explain savings, interference and long-term motor adaptation effects. *PLoS Comput Biol* 7: e1002210, 2011.
- Besser M, Kowalk D, Vaughan C.** Mounting and calibration of stairs on piezoelectric force platforms. *Gait Posture* 1: 231–235, 1993.
- Crisicimagna-Hemminger SE, Shadmehr R.** Consolidation patterns of human motor memory. *J Neurosci* 28: 9610–9618, 2008.
- Diedrichsen J, Verstynen T, Lehman SL, Ivry RB.** Cerebellar involvement in anticipating the consequences of self-produced actions during bimanual movements. *J Neurophysiol* 93: 801, 2005.
- Donchin O, Francis JT, Shadmehr R.** Quantifying generalization from trial-by-trial behavior of adaptive systems that learn with basis functions: theory and experiments in human motor control. *J Neurosci* 23: 9032, 2003.
- Galea JM, Vazquez A, Pasricha N, de Xivry JJ, Celnik P.** Dissociating the roles of the cerebellum and motor cortex during adaptive learning: the motor cortex retains what the cerebellum learns. *Cereb Cortex* 21: 1761–1770, 2011.
- Heng C, de Leon RD.** The rodent lumbar spinal cord learns to correct errors in hindlimb coordination caused by viscous force perturbations during stepping. *J Neurosci* 27: 8558–8562, 2007.
- Huang VS, Haith A, Mazzoni P, Krakauer JW.** Rethinking motor learning and savings in adaptation paradigms: model-free memory for successful actions combines with internal models. *Neuron* 70: 787–801, 2011.
- Ilg W, Giese M, Gizewski E, Schoch B, Timmann D.** The influence of focal cerebellar lesions on the control and adaptation of gait. *Brain* 131: 2913–2927, 2008.
- Ingram JN, Howard IS, Flanagan JR, Wolpert DM.** A single-rate context-dependent learning process underlies rapid adaptation to familiar object dynamics. *PLoS Comput Biol* 7: e1002196, 2011.
- Jayaram G, Tang B, Pallegadda R, Vasudevan EV, Celnik P, Bastian A.** Modulating locomotor adaptation with cerebellar stimulation. *J Neurophysiol* 107: 2950–2957, 2012.
- Joiner WM, Smith MA.** Long-term retention explained by a model of short-term learning in the adaptive control of reaching. *J Neurophysiol* 100: 2948, 2008.
- Kawato M, Furukawa K, Suzuki R.** A hierarchical neural-network model for control and learning of voluntary movement. *Biol Cybern* 57: 169–185, 1987.
- Kojima Y, Iwamoto Y, Yoshida K.** Memory of learning facilitates saccadic adaptation in the monkey. *J Neurosci* 24: 7531–7539, 2004.
- Kording KP, Tenenbaum JB, Shadmehr R.** The dynamics of memory as a consequence of optimal adaptation to a changing body. *Nat Neurosci* 10: 779–786, 2007.
- Krakauer JW, Ghez C, Ghilardi MF.** Adaptation to visuomotor transformations: consolidation, interference, and forgetting. *J Neurosci* 25: 473–478, 2005.
- Lee JY, Schweighofer N.** Dual adaptation supports a parallel architecture of motor memory. *J Neurosci* 29: 10396–10404, 2009.
- Malone LA, Vasudevan EV, Bastian AJ.** Motor adaptation training for faster relearning. *J Neurosci* 31: 15136–15143, 2011.
- Maschke M, Gomez CM, Ebner TJ, Konczak J.** Hereditary cerebellar ataxia progressively impairs force adaptation during goal-directed arm movements. *J Neurophysiol* 91: 230–238, 2004.
- Mawase F, Haizler T, Bar-Haim S, Karniel A.** Kinetic adaptation during locomotion on a split-belt treadmill. *J Neurophysiol* 109: 2216–2227, 2013.
- Miall RC, Christensen LO, Cain O, Stanley J.** Disruption of state estimation in the human lateral cerebellum. *PLoS Biol* 5: e316, 2007.
- Morton SM, Bastian AJ.** Cerebellar contributions to locomotor adaptations during splitbelt treadmill walking. *J Neurosci* 26: 9107–9116, 2006.
- Morton SM, Bastian AJ.** Cerebellar control of balance and locomotion. *Neuroscientist* 10: 247–259, 2004.
- Pekny SE, Criscimagna-Hemminger SE, Shadmehr R.** Protection and expression of human motor memories. *J Neurosci* 31: 13829–13839, 2011.
- Reisman DS, Block HJ, Bastian AJ.** Interlimb coordination during locomotion: what can be adapted and stored? *J Neurophysiol* 94: 2403–2415, 2005.
- Reisman DS, Wityk R, Silver K, Bastian AJ.** Locomotor adaptation on a split-belt treadmill can improve walking symmetry post-stroke. *Brain* 130: 1861–1872, 2007.
- Robinson FR, Soetedjo R, Noto C.** Distinct short-term and long-term adaptation to reduce saccade size in monkey. *J Neurophysiol* 96: 1030–1041, 2006.
- Roerdink M, Coolen B, Clairbois B, Lamoth CJ, Beek PJ.** Online gait event detection using a large force platform embedded in a treadmill. *J Biomech* 41: 2628–2632, 2008.
- Scheidt RA, Reinkensmeyer DJ, Condit MA, Rymer WZ, Mussa-Ivaldi FA.** Persistence of motor adaptation during constrained, multi-joint, arm movements. *J Neurophysiol* 84: 853, 2000.
- Scheidt RA, Stoeckmann T.** Reach adaptation and final position control amid environmental uncertainty after stroke. *J Neurophysiol* 97: 2824–2836, 2007.
- Shadmehr R, Brashers-Krug T.** Functional stages in the formation of human long-term motor memory. *J Neurosci* 17: 409–419, 1997.
- Shadmehr R, Mussa-Ivaldi FA.** Adaptive representation of dynamics during learning of a motor task. *J Neurosci* 14: 3208–3224, 1994.
- Shmuelof L, Krakauer JW.** Are we ready for a natural history of motor learning? *Neuron* 72: 469–476, 2011.
- Smith MA, Ghazizadeh A, Shadmehr R.** Interacting adaptive processes with different timescales underlie short-term motor learning. *PLoS Biol* 4: e179, 2006.
- Thoroughman KA, Shadmehr R.** Learning of action through adaptive combination of motor primitives. *Nature* 407: 742–747, 2000.
- Tseng Y, Diedrichsen J, Krakauer JW, Shadmehr R, Bastian AJ.** Sensory prediction errors drive cerebellum-dependent adaptation of reaching. *J Neurophysiol* 98: 54–62, 2007.
- Zarahn E, Weston GD, Liang J, Mazzoni P, Krakauer JW.** Explaining savings for visuomotor adaptation: linear time-invariant state-space models are not sufficient. *J Neurophysiol* 100: 2537–2548, 2008.